NeuroImage 285 (2024) 120479

Contents lists available at ScienceDirect

NeuroImage

journal homepage: www.elsevier.com/locate/ynimg

Technical Note

An easy-to-implement, non-invasive head restraint method for monkey fMRI

Reiji Tanaka [a,b,1], Kei Watanabe [a,c,d,1,*], Takafumi Suzuki [a,d], Kae Nakamura [e], Masaharu Yasuda [e], Hiroshi Ban [a,d], Ken-ichi Okada [f], Shigeru Kitazawa [a,c,d]

[a] Graduate School of Frontier Biosciences, Osaka University, Osaka 565-0871, Japan
[b] Japan Society for the Promotion of Science (JSPS), Tokyo, Japan
[c] Graduate School of Medicine, Osaka University, Osaka 565-0871, Japan
[d] Center for Information and Neural Networks, National Institute of Information and Communications Technology, Osaka 565-0871, Japan
[e] Department of Physiology, Kansai Medical University, Osaka 573-1010, Japan
[f] School of Medicine, Hokkaido University, Sapporo 060-8638, Japan

ARTICLE INFO

Keywords:
Monkey
fMRI
non-invasive

ABSTRACT

Functional magnetic resonance imaging (fMRI) in behaving monkeys has a strong potential to bridge the gap between human neuroimaging and primate neurophysiology. In monkey fMRI, to restrain head movements, researchers usually surgically implant a plastic head-post on the skull. Although time-proven to be effective, this technique could create burdens for animals, including a risk of infection and discomfort. Furthermore, the presence of extraneous objects on the skull, such as bone screws and dental cement, adversely affects signals near the cortical surface. These side effects are undesirable in terms of both the practical aspect of efficient data collection and the spirit of "refinement" from the 3R's. Here, we demonstrate that a completely non-invasive fMRI scan in awake monkeys is possible by using a plastic head mask made to fit the skull of individual animals. In all of the three monkeys tested, longitudinal, quantitative assessment of head movements showed that the plastic mask has effectively suppressed head movements, and we were able to obtain reliable retinotopic BOLD signals in a standard retinotopic mapping task. The present, easy-to-make plastic mask has a strong potential to simplify fMRI experiments in awake monkeys, while giving data that is as good as or even better quality than that obtained with the conventional head-post method.

1. Introduction

Functional magnetic resonance imaging (fMRI) in behaving monkeys has become increasingly popular in cognitive neuroscience (Vanduffel et al., 2001; Ku et al., 2011). It has a potential to bridge the gap between human fMRI and monkey electrophysiology studies. However, there are still several problems that need to be solved in monkey fMRI, which could discourage those interested in this field from participating in it. These problems include motion artifacts caused by head and body movements, magnetic field susceptibility caused by head-restraint implants, and signal dropout caused by an air-filled gap along the body margin (e.g., back of the neck). To overcome these problems, researchers have long strived to develop effective protocols; these include optimization of the seating posture (Logothetis et al., 1999; Miyamoto et al., 2017), use of a contrast-enhancing agent (Vanduffel et al., 2001), optimization of coil position, the direction of phase-encoding, and the implant type and location (Srihasam et al., 2010; Oritz-Rios et al., 2018).

The present report describes a novel method for head restraint of awake monkeys in an MRI scanner using only a plastic head mask. This mask is easy to make and does not require any invasive procedures. In behavioral neurophysiology, a previous report has described the effectiveness of plastic masks for head-restraint in neuronal recording in awake monkeys (Drucker et al., 2015). By refining this method, we have found that a plastic mask can be used in fMRI experiments, which require tighter head restraint than neurophysiological experiments. The present plastic head mask is made of a standard thermoplastic splint material that is softened by hot water so that it can be deformed. It was molded so that it conformed to the contours of the animal's scalp (skull),

* Corresponding author at: Graduate School of Frontier Biosciences, Osaka University, Osaka 565-0871, Japan.
E-mail address: kei_watanabe@fbs.osaka-u.ac.jp (K. Watanabe).
[1] These authors contributed equally to this work.

https://doi.org/10.1016/j.neuroimage.2023.120479
Received 24 July 2023; Received in revised form 15 November 2023; Accepted 28 November 2023
Available online 29 November 2023

zygomatic bones and occipital ridge. No surgical implant was required from the early acclimatization process to the behavioral scan sessions.

The present technique has several advantages over the conventional invasive head-post method. First, since no surgical procedures are required, there is no risk of infection or pain from surgical wounds, thus greatly reducing the stress on animals. This not only conforms to the spirit of the 3R's, but could also mean that a lower level of pain could be declared in the ethical review for animal experiments. Second, because the monkey's head, from the surface of the brain to the scalp, is kept completely intact, the BOLD signal is free of artifact-related (implant-derived) noise. Third, because the material needed to create one head mask (i.e., one piece of commercially available splint material) costs only about 50 US dollars and because it requires only a single brief general anesthesia session (about 30–40 min) to make one head mask, the cost and time required for this method are less than those in the conventional methods that require surgery.

Using the plastic mask, we trained three monkeys in a fixation task for retinotopic mapping. All of them rarely showed abrupt head movements that appeared as spikes in an x, y or z translation plot in the post-hoc image realignment. We were able to obtain reliable retinotopic BOLD responses in the standard visual meridian localizers. The present study demonstrates that the use of a non-invasive plastic mask works well in fMRI experiments in awake monkeys. We describe points to consider in creating a mask that effectively suppresses head movement.

2. Materials and methods

2.1. Subjects

We used three female Japanese monkeys (Macaca fuscata, monkeys B, R and T): 7, 5 and 5 years old weighing 6, 7 and 6 kg, respectively. None of the monkeys had any head-post implants before or during this study. Monkey B had 9 months of daily training in a mock scanner prior to the scan. During this 9-month period, monkey B was used to optimize

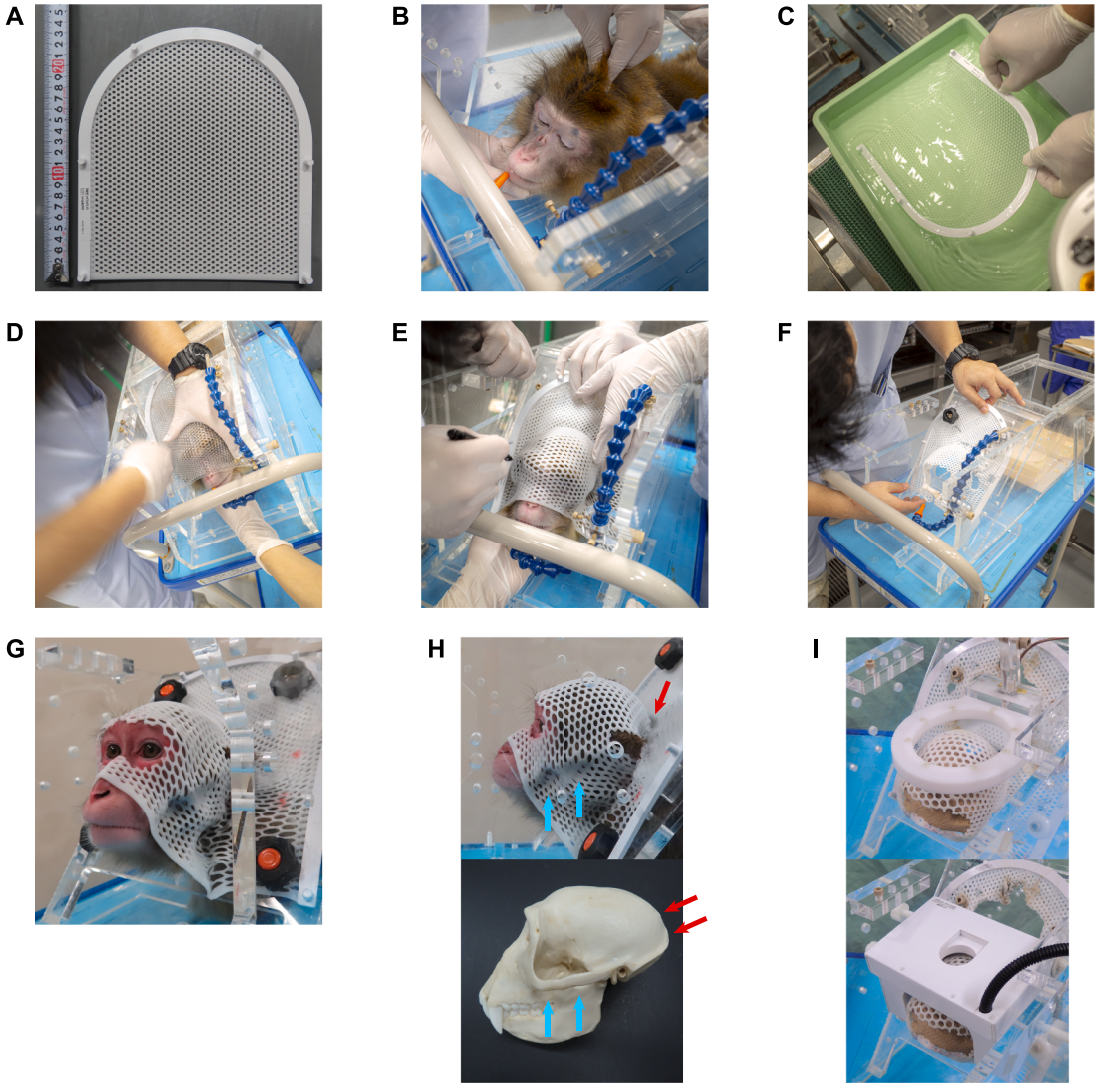

Fig. 1. Mask preparation procedure.
(A) Plastic splint material used to make a mask. (B) The head of an anaesthetized monkey was set in the same position as in the usual experiment. (C) Splint material immersed in hot water (> 90 °C). (D) The moment when the softened splint material was pressed against the monkey's head after cooling (< 50 °C). Note that one person grasped the monkey's jaw and tried to keep the monkey's head still, while the other person shaped the splint material. (E) Cutting lines drawn by a permanent marker. (F) The mask was attached to a chair using M6 screws to check its compatibility with the chair. (G) Front view of a monkey restrained by the plastic mask. (H) Side view of a monkey (top) and a model of the corresponding scalp (bottom). Note that in the good mask, the splint material was bent to perfectly conform to the shapes of the zygomatic bones (cyan arrows) and the occipital ridge (red arrows). (I) Two types of receiver coils used in the present study. By making the shape of the mask closely fit the monkey's head, various types of coils could be placed close to the monkey's head.

the present plastic mask method. Monkeys R and T were trained daily for 3 months before the scan. For these two monkeys, training was carried out according to a pre-planned training regimen which we developed based on prior experience with monkey B. The experimental procedures were approved by the Animal Research Committee at the Graduate School of Frontier Biosciences, Osaka University, and were in full compliance with the guidelines of the National BioResource Project "Japanese Macaques" and the National Institutes of Health guide for the care and use of Laboratory animals.

2.2. Plastic mask details

The plastic mask for head immobilization was made using a medical plastic splint material (Fig. 1A) (product number: MTAPUR, 3.2-mm thick, CIVCO Radiotherapy, Orange City, IA) which is usually used to inhibit body movements of human patients during radiotherapy treatment. For monkey T, as we discuss later, part-way through the fMRI data collection, we remade the mask using more solid material (product number: MTAPUIR2232, 3.2-mm thick, CIVCO Radiotherapy, Iowa). To make plastic masks, we first anaesthetized a monkey with medetomidine (0.1 mg/kg, i.m.) and ketamine (2.5 mg/kg, i.m.) and placed it on a horizontal MRI chair (Fig. 1B). We manually fixed the monkey's head at the desired height and axial location (Fig. 1B). Since, in an anaesthetized monkey, the head position tends to sink lower than the usual position at which the monkey faces a screen and sucks a drinking spout during the experiment, we recommend pre-fixing a drinking spout to the chair at the height normally used by monkeys, and to manually hold the monkey's head at that position until the entire production process is completed (Fig. 1B).

While one person held the head of the monkey, another soaked one piece of the U-shaped splint material in boiling water ($> 90\ ^{\circ}C$) until it was softened (1, 2 min) (Fig. 1C). Before the softened splint material was applied to the monkey, it was quickly dried with paper towels and cooled to under 50 °C. The softened material was placed directly on the monkey's head with the straight end of the U-shaped material placed at the level of the monkey's nose, and molded by hand to fit the contours of the monkey's scalp (skull), zygomatic bones and occipital ridge (Fig. 1D). Even after the initial shape of the plastic mask was determined, we held the splint material and the monkey's head firmly in place for a few minutes until the splint material cooled and hardened. After the material regained its stiffness, we used a permanent marker pen to draw cut-here lines on the area of the mask covering the eyes and ears. We also marked the locations at the base of the mask where the M6 screws would penetrate to contact screw holes on the monkey chair (Fig. 1E). We fixed the mask to the chair with four M6 screws (top, bottom, left and right of the protruding part of the monkey head of the mask). During a single anesthesia session in one monkey (about 30–40 min), we would usually make two to three masks, and we selected the best one among them. After returning the monkey to the cage, we verified that the selected mask could be fitted to the chair with four M6 screws (Fig. 1F).

We selected the mask based on the following criteria: (1) the mask did not interfere with head coils; (2) the monkey did not show any signs of discomfort when wearing the mask; (3) the mask did not bend when the monkey moved its lower body; and (4) movement of the head when drinking from spout was minimal (i.e., slight jaw movements during drinking did not propagate to the top of the head. This is usually achieved by not completely covering the lower jaw with the mask).

On the following day, we put the monkey on the chair without anesthesia and checked the fitting of the mask (Fig. 1G). If there were places that were too tight or loose, we took the mask off the monkey and used a soldering iron to partially soften and deform the mask. We then put the mask back on the monkey and checked the fit. Once it was confirmed that the mask fit the monkey's head tightly, task training began from the next session. We did not shave or trim the monkey's fur. No side effects such as swelling or bruising were observed after more than one year of use.

2.3. Optimal shape of the mask

To minimize head movement during experiments, it is critical to fit the mask to the shape of the monkey's head as tight as possible. Through trial-and-error, we found two critical locations on the skull: the zygomatic bones and the occipital ridge (Fig. 1H, cyan and red arrows, respectively). Pressing the softened thermoplastic tightly against the contours of the zygomatic bones and the occipital ridge is crucial for achieving an optimal fit of the mask. Fig. 1H shows an example of how these two locations are molded as closely as possible relative to the monkey's head. In this mask, the plastic is firmly pressed just below the zygomatic bones (cyan arrows). This tight fit prevents the zygomatic bones from being displaced upward and downward from their original position in the mask. The plastic tightly adheres to the occipital ridge, leaving a gap between the occipital area and the neckplate of the chair (red arrows). This portion of the splint on the occipital ridge held the head down from above.

Fitting the mask optimally around the monkey's head not only reduces head movement, but also allows the head coil to be positioned as close as possible to the monkey's head. Fig. 1I shows the two different types of coils we used. We were able to bring both coils close enough to the monkey's head to acquire EPI images of the whole brain. Use of the optimally shaped mask allows placement of a multichannel coil as close to the head as possible (Fig. 1I, bottom).

2.4. Details of head-post implants used for comparison with the plastic mask

To assess the quality of fMRI images obtained with the plastic mask, we compared the images with those obtained in another monkey whose head was restrained by a standard PEEK head-post. The fMRI images of this monkey were obtained in a different experiment prior to the present study in our laboratory.

The head post was designed at the National Institute for Physiological Sciences (Okazaki, Japan) and manufactured by a workshop in Osaka University. The head post had a trapezoidal cross-section (top 15 mm, bottom 20 mm, height 15 mm) and a height of 35 mm. This trapezoidal column was connected at its bottom to a disk-shaped base 26 mm in diameter and 10 mm high. This disk-shaped base was placed directly on the skull with its center located at stereotaxic coordinates of AP 15.5 mm and ML 0 mm. The bone screws were commercially-available pan head screws (M3L5) made of PEEK (part number PE-0305, Wilco Inc. Yokohama, Japan). We implanted 18 of these from the occipital to the temporal region of the skull as anchors for dental cement.

2.5. Training

Behavioral training was conducted 5 days per week outside the scanner. Access to water was restricted in the monkeys' home cages except for weekends. The monkeys sat in a custom-made horizontal primate chair in a "sphinx" position in a mock MR bore placed in a dimly lit, sound-attenuated cubicle. Visual stimuli were presented on a standard 19-in. TFT monitor (DELL) placed 56 cm from the monkey's face. Eye movements were monitored at 120 Hz using an infrared eye tracking system (EyeLink 1000, SR Research). MATLAB Psychtoolbox was used to present stimuli, control the task events and acquire behavioral data.

Training was conducted in a step-by-step manner (Fig. 2A,B). After the monkeys were acclimated to head-restraint by the plastic mask and trained to drink from a spout (termed "acclimatization to head-restraint" and "spout-training"), calibration for eye movement tracking was conducted ("calibration"). Subsequently, the monkeys were trained in a standard fixation task ("fixation task (trial-by-trial)") and in a continuous version of the fixation task in which fixation point (FP) was presented continuously for 2–4 min. To encourage continuous fixation

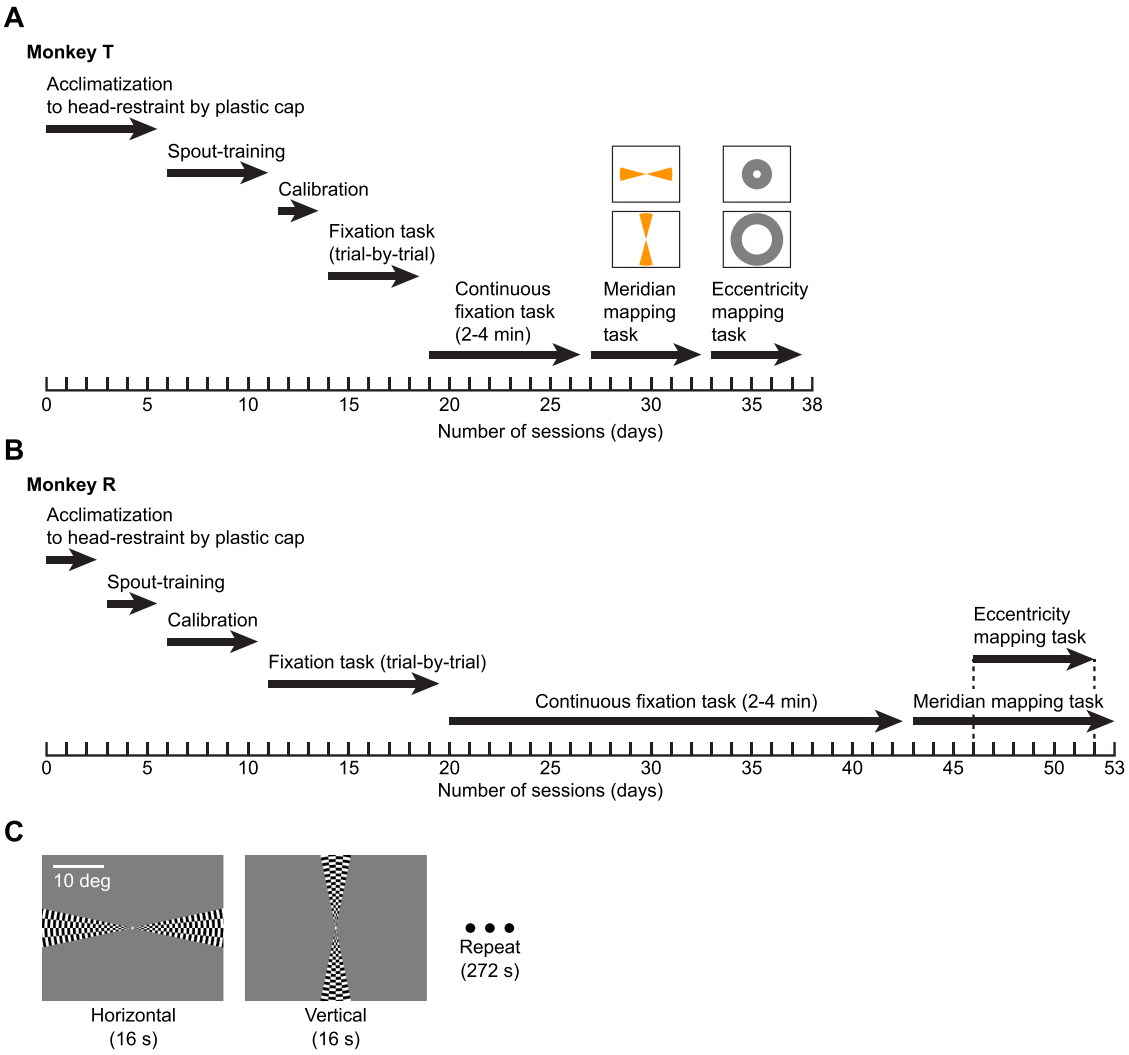

Fig. 2. Step-by-step training regimen in pre-scan training.
Progress of pre-scan training in monkey T. (B) Same as in A, but for monkey R. (C) The visual stimuli for the horizontal and vertical meridian mapping. In the actual experiments, chromatic checkerboard (red/green and blue/yellow) patterns were also presented. A scale bar indicates visual angle.

within a square fixation window (6.1° on a side), rewards (drop of fruit juice) were given while their gaze was in the window, and the inter-reward interval was shortened step-wise from 2500 ms to 500 ms as fixation continued without a fixation break (FB). When the monkey made a FB, the inter-reward interval was reset to the initial value (2500 ms). After fixation performance reached an asymptote (about 90 %), visual stimuli were presented for the standard visual meridian and eccentricity localizer scans (wedge and annulus stimuli) were added to the fixation task (see below).

We used a relatively large fixation window compared to those which are often used in vision neuroimaging studies (e.g., 2.0° on a side), but not because there was a problem with measuring eye movement or a problem with head stability when we used the plastic mask. Instead, this was because the ultimate goals of our monkey fMRI experiments were to study brain activity in cognitive tasks (which usually involve a fixation window larger than those used in visual experiments) and brain activity during free viewing of various visual stimuli. For these purposes, it was not necessary for us to make the fixation window smaller than necessary. In addition, we confirmed that although we used a relatively large fixation window (6.1° × 6.1°), the monkeys' gaze location during the fixation task was located predominantly within a smaller, imaginary 2.0° × 2.0° fixation window (see Supplementary Fig. 1B and the corresponding section in the Results).

2.6. MR data acquisition

The blood oxygen level-dependent (BOLD) signal was measured by the echo planner imaging (EPI) method using a 3T Magnetom Prisma-Fit MRI scanner (Siemens, München, Germany). A custom-made phased-array 12-ch receiver coil (Takashima Seisakusho Co., Ltd., Tokyo, Japan) was fitted around the mask, covering the entire brain of the monkey. Each daily session consisted of three or four functional scans which we called "runs". Each run lasted 272 s, using the following parameters: repetition time (TR) = 2 s; echo time (TE) = 30 ms; flip angle = 75°; 86 × 86 matrix; voxel size = 1.5 mm isotopic; 62 slices; and phase encoding direction (PE) = anterior/posterior (A/P). For the image distortion correction (topup processing), five EPI images of PE = P/A were also obtained in each session. The first eight volumes of each run were discarded to cut off initial steady-state problems.

In a separate session, higher resolution T1-weighted anatomical images were obtained with monkeys anaesthetized by medetomidine (0.03 mg/kg, i.m.), midazolam (0.2 mg/kg, i.m.) and butorphanol tartrate (0.3 mg/kg, i.m.). We used a 1-channel loop coil (Takashima Seisakusho Co., Ltd.) and the following parameters: TR = 1.5 s; TE = 1.92 ms; flip angle = 8°; 192 × 192 matrix; voxel size = 0.67 mm isotopic; and 192 slices. Six, three and four structural scans were taken for monkeys B, R and T, respectively, and averaged for each monkey.

2.7. Visual stimuli

Inside the MRI scanner, visual stimuli were backprojected to a screen placed 56 cm from the monkey's eyes. The size of the projection was 34.9° × 28.3° of visual angle (1280 × 1024 pixels). During stimulus presentation, the monkeys maintained fixation within a 6.1° × 6.1° window centered on a white dot (0.23° × 0.23°) displayed in the center of the screen with a gray background. Inside the scanner, eye movements were monitored at 60 Hz by an MRI-compatible infrared eye tracking system (LiveTrack AV for fMRI v2, Cambridge Research Systems, Rochester, U.K.).

In the visual meridian mapping, we used the standard stimuli to map the cortical representation of the visual field in human and non-human primates (Wandell et al., 2007; Kolster et al., 2014). Around the FP, two checkerboard wedges with 24° angle were flickered in counterphase at 4 Hz (i.e., each wedge was replaced every 250 ms) (Fig. 2C). The combinations of checkerboard colors were black/white, red/green and blue/yellow. The wedges were presented to the right and left of the FP in the horizontal blocks, and above and below the FP in the vertical blocks. The duration of each block was 16 s. The horizontal and vertical blocks were alternately presented throughout the entire period of each MRI run (272 s) (Horizontal: 9 blocks, Vertical: 8 blocks). As in the training outside the scanner, the monkey received liquid rewards for successful fixation to the FP. Continuous fixation shortened the inter-reward intervals to motivate longer stable fixation.

3. Data analysis

3.1. FMRI data preprocessing

Acquired EPI images were processed using the Functional MRI of the Brain (FMRIB) Software Library (FSL; https://fsl.fmrib.ox.ac.uk/fsl/fslwiki; Smith et al., 2004) and SPM12 software (The Wellcome Centre for Human Neuroimaging; https://www.fil.ion.ucl.ac.uk/spm/; Ashburner, 2012). Initially, using volumes acquired at PE = P/A, FSL's topup processing was applied to all experimental EPI volumes (taken at PE = A/P) to correct for susceptibility induced distortions (Andersson et al., 2003). EPI volumes were then preprocessed using SPM12 as follows: (1) slice timing correction; (2) realignment for compensation for head motions using the first volume as a reference; (3) spatial smoothing by a Gaussian kernel with a 2.0-mm full-width at half maximum. Coregistration processing was applied to the anatomical T1 image and the averaged image of realigned EPI volumes, and the activation maps were overlaid on the T1 image.

3.2. Functional image analysis

Statistical analysis of brain activation was performed by SPM12. The activation of each voxel was modeled by a general linear model (GLM) with the standard hemodynamic response function (HRF) implemented in SPM12. We used the following regressors: (1) Horizontal wedge presentation period; (2) Vertical wedge; (3) Reward; (4) Saccade; (5) Blink. Additionally, 6 covariates modeling head movements were also included as nuisance regressors. We defined saccades as eye movements with a maximum velocity exceeding 80°/s. The onset and offset of a saccade were defined as the points at which eye velocity exceeded and fell below 40°/s, respectively. These criteria were determined based on previous studies (Berg et al., 2009; Ito et al., 2013). We defined blinks as periods during which either the pupil center or corneal reflection (the two measures used for the detection of eye movement) could not be detected. Among these periods, we regarded those of less than 50 ms as not blinks but rather as a momentary lapse in detection. This is because completion of an eye blink usually takes more than 100 ms (Goldstein et al., 1992; Tada et al., 2013). The eye-position data in these momentary lapses were linearly interpolated.

Each regressor was a convolution of the HRF with a boxcar-model that took the value of 1 during the occurrence of each event and 0 otherwise. *T*-tests were applied to the estimated GLM's parameters of each voxel, and we defined the voxels that exceeded the threshold of $p < 0.005$ (corrected by family-wise error cluster level correction; FWEc) as significantly activated voxels. Inflated and flattened maps of brain activation were generated for each monkey by Caret5 (https://www.nitrc.org/projects/caret/; Van Essen et al., 2001).

3.3. Movement estimation

Movement of monkey's head during scans was estimated by the "realignment" function in SPM12. For each volume, the realignment function estimated the values of translation and rotation relative to the first volume of each run. We call these values "cumulative movements" which represent the displacement of the image position at each time point relative to that in the first volume in each run. We also calculated the spatial displacement between two consecutive EPI images (taken every 2.0 s) and call these values "relative movements". To quantitatively assess the stability of head restraint, we constructed relative frequency histograms of the relative movements in the three monkeys used in this study (Fig. 4C–E). We fitted these histograms to a gamma distribution function, with mode and SD used as measures of central tendency and variability, respectively. This is because the histograms in Fig. 4C–E were substantially positively skewed, and therefore it was not appropriate to use the mean as a representative value (measure of central tendency) for these datasets (i.e., it is not appropriate to fit Gaussian models). Rather, the shape of the graph seemed to be best fit by a gamma distribution function. There are two parameters in a gamma distribution: shape parameter k and scale parameter θ. For gamma distributions with a small k value, the mode rather than the mean is considered to be a more appropriate measure of central tendency. Note that the median of a gamma distribution, as a function of its shape parameter k, has no known representation in terms of elementary functions (i.e., the median cannot be calculated using a simple function). In the present case, because the obtained k values were small, we chose the mode as a measure of central tendency. The standard deviation (SD) in gamma distributions is calculated as $\sqrt{k}\theta$.

4. Results

4.1. Progress of pre-scan training

Training was conducted in a step-by-step manner. Of the three monkeys, we report the progress of monkeys R and T, who underwent a similar, pre-planned training regimen that was developed based on our experience with monkey B (the first monkey used in this study). For monkey B, pre-scan training lasted about 9 months. This period was focused on the optimization of various experimental elements, including optimization of the shape of the plastic mask, stimulus presentation and eye movement measurements in the scanner.

Both monkeys R and T learned the fixation task (continuous fixation for 2–4 min) quickly (monkey R, 42 sessions, about 9 weeks; monkey T, 26 sessions, about 6 weeks) from the start of training with head-restraint (Fig. 2A,B). The monkeys were then trained on the visual meridian mapping task (Fig. 2C) and the visual eccentricity mapping task. Again, both monkeys learned these two tasks quickly; the monkeys learned to continue to gaze at the fixation point for more than 90 % of the intervals in one block (usually 4–5 min), while localizer stimuli were presented continuously. After training of the visual localizer tasks was complete, we began fMRI data acquisition.

4.2. Examination of fMRI data quality

We assessed the quality of the fMRI images obtained with the plastic mask (Fig. 3, termed "plastic mask monkey"). For comparison, we

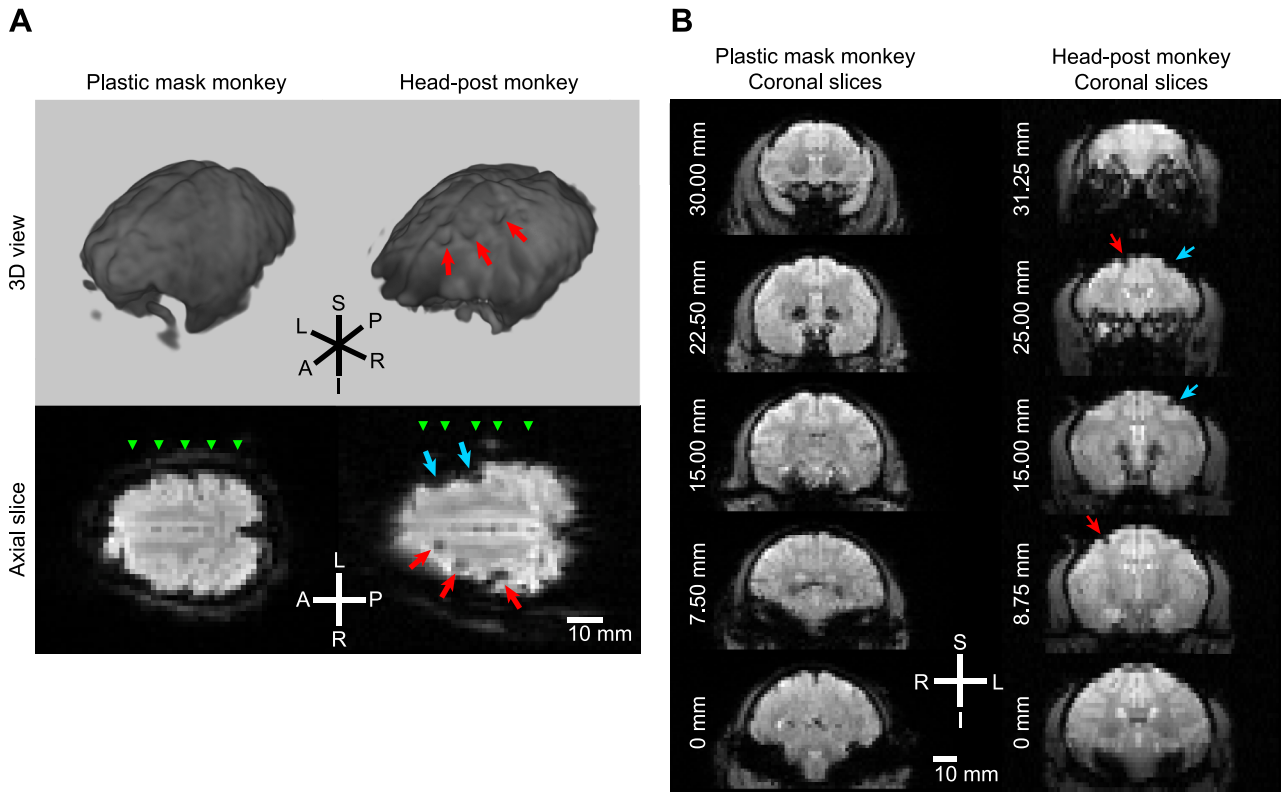

Fig. 3. Comparison of EPI images between the plastic mask and the head-post methods.
(A) The upper row shows 3D views of the brains reconstructed from EPI data. Left, data acquired with a plastic mask (monkey B, termed 'plastic mask monkey'). Right, data acquired with a head-post (monkey K, termed 'head-post monkey'). The bottom panels show axial slices 6.4 mm below the vertex in each monkey. Red and cyan arrows indicate signal drop near bone screw holes. Green triangles indicate AP positions of the slices presented in B. (B) Coronal slices of the two monkeys shown in A. The numbers on the left represent the distance from the most posterior slice of the five images for each monkey.

examined fMRI images of a monkey whose head was restrained by a standard PEEK head-post. The head-post was attached to the skull by PEEK bone screws and dental cement (Fig. 3, "head-post monkey"). The fMRI images of this monkey were obtained in a different experiment prior to the present study in our laboratory. The images of this head-post-restrained monkey showed highly noticeable signal drops and distortions near the cortical surface (Fig. 3A, red and cyan arrows). Although it is not the focus of this paper to determine what exactly caused these signal drops, visual inspection of these EPI images suggests that the adverse effects caused by the implant appear to originate mainly from bone screws; the BOLD signal was affected only near the bone screw holes in this monkey (Fig. 3B, right). These signal drops can prevent the fine-grained examination of brain activation near the cortical surface. Here, we do not intend to suggest that the head-post implant always has a negative effect on the BOLD signal. For example, the noise from the bone screw may be resolved by ensuring that the drill stops at the inner table of the skull when drilling the hole for the bone screw, and this may allow experimenters to obtain clean EPI images near the brain surface. However, this requires highly-advanced skills and a careful surgery. With the present method, because the plastic mask does not damage the skin or the skull at all, experimenters do not need to be highly skilled in surgical techniques. As shown in Fig. 3A left, with the plastic mask, there was no change in local magnetic susceptibility, and accordingly there were no signal drops or distortions near the cortical surface.

4.3. Examination of head movements

Next, we examined whether or not head movements during a fMRI scan were sufficiently suppressed by the plastic mask. Fig. 4A,B shows a representative example of the time-course of cumulative head movements in an experimental run which was calculated as the deviation from the first image obtained in this run (see **Materials and Methods**). These data were collected in the meridian mapping task in monkey B. The magnitude of head movements was estimated by the "realignment" function in SPM12. In Fig. 4A, the red, blue and green lines indicate translational movements in millimeters along superior-inferior (S-I), right-left (R-L) and anterior-posterior (A-P) axis, respectively. In Fig. 4B, the red, blue and green lines indicate estimated rotational movements in degrees (pitch, yaw and roll, respectively). The result showed that, for this experimental run, the cumulative movements were successfully suppressed to almost within 0.4 mm (translation) and 0.006° (rotation), except for a single occasion at around 245 s where A-P translational movement showed a spike of about 1.0 mm. According to our observation during the actual scan, this abrupt movement was caused by a large bodily movement accompanying a change in posture.

To confirm that the above result reflects an overall trend across animals, we examined the magnitude of relative movement (**Materials and Methods**) in the three monkeys while they performed the meridian mapping task (19 runs in 4 sessions in monkey T; 7 runs in 2 sessions in monkey B; 3 runs in 1 session in monkey R; each run lasted 272 s). Fig. 4C–E shows relative frequency histograms of the estimated relative movements in the three monkeys, with a best-fit gamma distribution function (red curve). The ordinate and abscissa illustrate relative frequency (%) and the magnitude of relative movement (mm), respectively. The results show that in all of the three monkeys, relative movement of greater than 1.0 mm scarcely occurred; the frequencies of such movement were 0.00 %, 0.32 % and 0.74 % in monkeys T, B and R, respectively. Here, the frequency was defined as the percentage of the relative movements exceeding 1 mm out of the total number of relative movement values (i.e., total number of volumes recorded across all

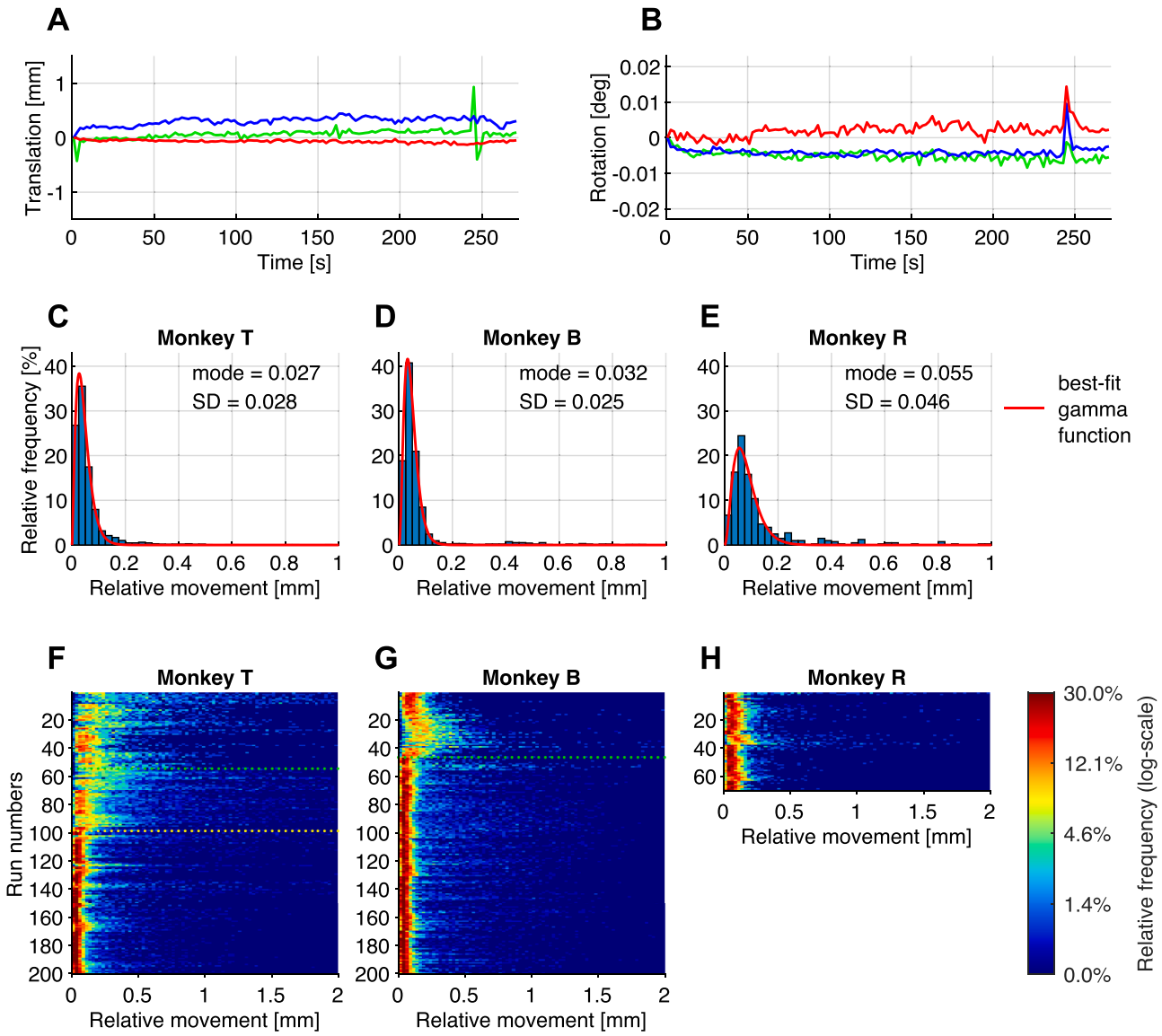

Fig. 4. Head movements during fMRI scans.
(A) Example of cumulative translational movements of the brain in millimeters in monkey B. Red, blue and green lines indicate the movements along the right-left, superior-inferior and anterior-posterior axes, respectively. The data were obtained during a single run of the meridian mapping task. (B) Same as in A, but for cumulative rotational movements in degrees. (C–E) Relative frequency histograms of relative movements (bin width = 0.025 mm) in each monkey during the meridian mapping task. The data were from the latest 19, 7 and 3 runs in monkey T, B and R, respectively. Red curves indicate gamma distribution function fit to each histogram, with peak point (mode) and standard deviation (SD) values. (F, G) Longitudinal record of the relative movement of individual monkeys throughout the experiment. The data in each horizontal row indicate a relative frequency histogram of relative movement in one run shown as a log-scale color map. The data are ordered from the first run (top of panels) to the last run (bottom). The data were obtained from all experimental runs in which monkeys were engaged either in continuous fixation (272 s/run, including the visual meridian task) or in free-viewing of movie clips of various natural scenes (300 or 360 s/run). Green dotted lines in monkeys T and B indicate the timing when we reshaped the mask for an improved fit to the zygomatic bones and the occipital ridges. For monkey T, we also changed the material of the mask to a more solid one. The yellow dotted line in monkey T indicates the timing when we adjusted the spout position. Runs that were interrupted due to hardware problems or the monkey's maladaptive behavior were excluded.

sessions minus one). For example, in monkey T, there were a total of 2565 relative movement values obtained in 19 runs. The resultant value of 0.00 % in monkey T indicates that there were no two consecutive volumes that exhibited relative movements of greater than 1.0 mm across all of the 19 runs in this monkey. The mode values (i.e., the magnitude of the most frequent relative movement) given by the best-fit gamma distribution function were 0.027, 0.032 and 0.055 mm, and the standard deviations were 0.028, 0.025 and 0.046 mm for monkeys T, B and R, respectively.

There have been various studies on the effects of head movements in fMRI (Friston et al., 1996). In many cases, movements within about the size of a voxel (1.5 mm in the present study) were regarded as acceptable (Czisch et al., 2004; Zou et al., 2008). Thus, the present results indicate that the plastic mask achieved a sufficient degree of head immobilization for clean fMRI data acquisition in awake monkeys, though during the course of fMRI scans, we noticed that there was a slight difference in the degree of immobilization among the three monkeys. Specifically, in earlier sessions, monkey T tended to show large head movements. For this monkey, we further examined whether its head movements could be better controlled by some remedial measures.

We made two changes and assessed the effect of these changes: a change in the material used to make the mask and a change in the position of the drinking spout. Fig. 4F–H illustrates changes in the frequency of relative movement over the entire experimental period in

each monkey. In each panel, the data in a horizontal row illustrate a relative frequency histogram of relative movement in one run. As we noted above, monkey T showed somewhat frequent head movements in early runs (Fig. 4F, up to about the 50th run). This was likely caused by a habit of this monkey to make frequent jaw movements upon receiving rewards from the spout. Thus, we decided to increase the strength of the mask material and adjust the position of the spout. A green dotted line in the results of monkey T (between runs 54 and 55) indicates the timing when we remade the mask by using more solid material for better stability (see **Materials and Methods**). We also took extra care to fit the new material as tight as possible around the zygomatic bones and the occipital ridge.

A yellow dotted line (between runs 98 and 99) indicates the timing when, through trial-and-error and visual inspection, we found the optimal position of the drinking spout where monkey T appeared to show the least jaw movements associated with drinking. The results showed that these modifications had positive effects. Regarding the change in the mask material, although some adjustment period (runs 55–64) was required for the monkey to get used to a new, stiffer mask, compared to the old mask, the new mask reduced the mode and SD values of relative movement from 0.14 to 0.064 mm and from 0.16 mm to 0.074 mm, respectively (data are from runs 45–54 for the old mask and runs 70–79 for the new mask). Subsequently, optimization of the spout position further reduced head movements. Between before and after optimization, the mode and SD values changed from 0.095 to 0.048 mm and from 0.12 to 0.056 mm, respectively (data are from runs

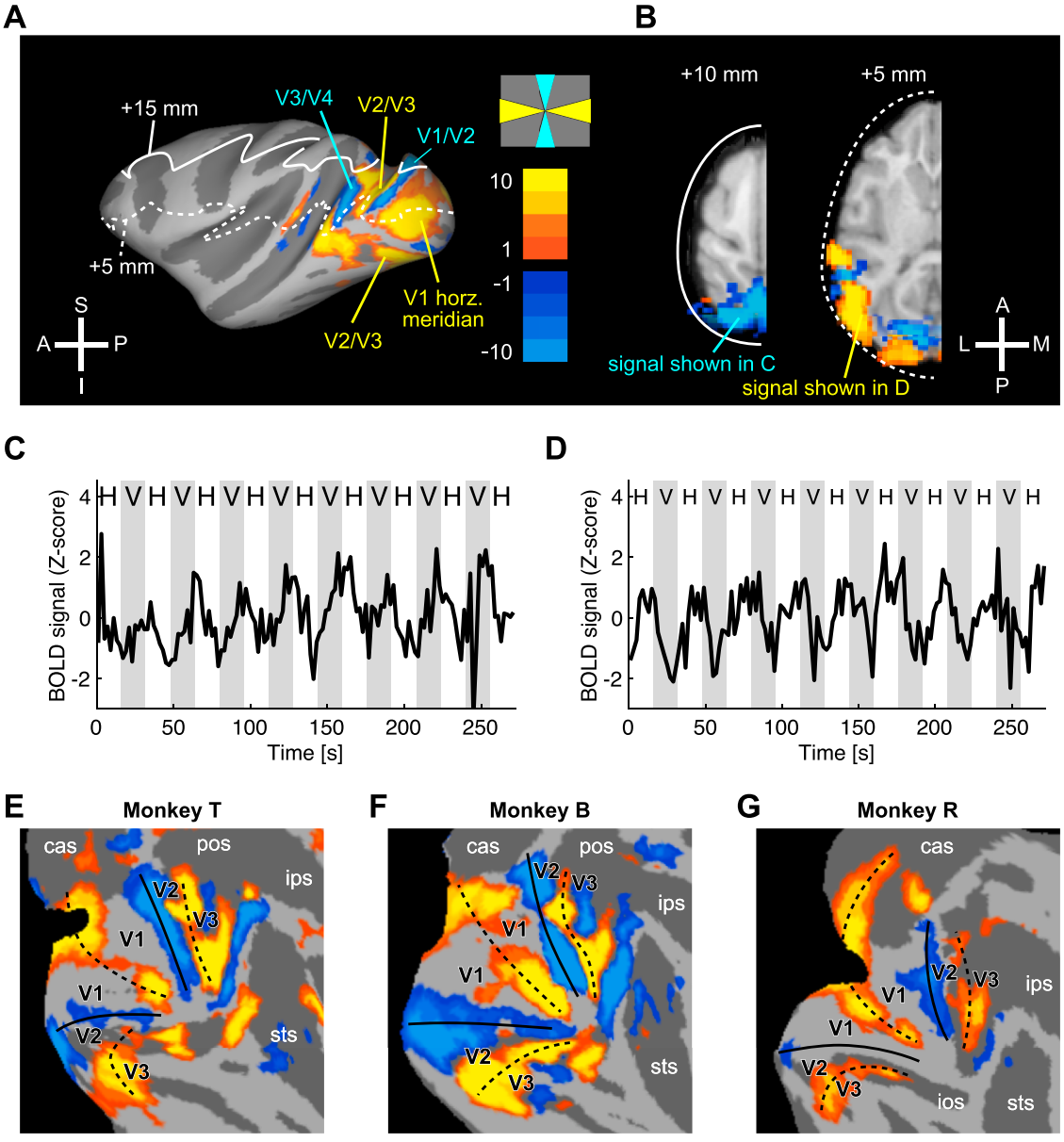

Fig. 5. Activation of the borders of early visual cortices.
(A) Cluster-corrected t-statistics map of voxels that were significantly activated by either the vertical (cold colors) or horizontal (warm colors) wedges ($p < 0.005$, FWEc) overlayed on the cortical surface. Two white lines indicate the positions of axial slices shown in B (+15 mm and +5 mm slices relative to the AC-PC plane. (B) Axial slices of the left hemisphere taken at the levels shown in A. (C) Time-course of BOLD signal modulation in one representative voxel taken from the cluster shown in the left panel in B. The cluster was activated by vertical wedges. The background colors of the plot area correspond to the orientations of wedges presented during that period (white: horizontal wedge, 'H'; gray: vertical wedge, 'V'). (D) Same as in **C**, but for a voxel taken from the cluster shown in the right panel in B which was activated by the horizontal wedges. (E–G) Flat map display of brain areas in individual monkeys that were significantly activated by the wedges (right hemisphere, $p < 0.005$, FWEc). The color codes were the same as in A. The dashed and solid black lines indicate the estimated borders of visual areas.

89–98 before optimization, and runs 99–108 after optimization).

For monkey B (Fig. 4G, green dotted line), although this monkey did not have a head movement issue, we remade the mask for a better fit to achieve a greater degree of head immobilization. For this monkey, we did not change the material used to create the mask. Between before and after the remake (runs 37–46 and 47–56, respectively), the mode and SD values changed from 0.11 to 0.039 mm and from 0.12 to 0.057 mm, respectively. This improvement is clearly visible in Fig. 4G. These results suggest that, for monkeys that move their heads frequently, the size and frequency of head movements can be reduced by either changing the mask material to increase its rigidity or adjusting factors other than the mask (spout position in the present case) or both.

Since the monkeys certainly would have become more acclimatized to the fMRI environment after each session, not only the remake of the mask and the adjustment of the spout position, but also a training effect should have contributed to the substantial improvement in head stability observed in Fig. 4F,G. Therefore, we suggest that the improvement of head stability can be ascribed to a combination of three factors: (1) a mask that fits better on the zygomatic bones and occipital ridge, (2) adjustment of the position of the drinking spout, and (3) a training effect.

4.4. Retinotopic mapping

To examine whether high-quality fMRI data can actually be obtained by the present method, in each of the three monkeys used in this study, we mapped the borders of the early visual areas (V1–V3) by independent visual stimulation of vertical and horizontal meridians (Rajimehr and Tootell, 2009; Kubilius et al., 2011; Lafer-Sousa and Conway, 2013) (**Materials and Methods**).

Significant retinotopic responses evoked by a pair of checkerboard wedges are shown in Fig. 5A,B. The cold colormap represents a vertical meridian and the warm colormap represents a horizontal meridian (Monkey B, left hemisphere, cluster-corrected t-statistic map, $p < 0.005$, FWEc). The result clearly reproduces the well-known symmetric retinotopic representations of the quadrant visual field in each of the early visual areas; the vertical wedge stimuli activated the boundaries of V1 and V2, and V3 and V4. The horizontal stimuli activated the boundary of V2 and V3, and the areas in V1. This result was obtained in 19, 7 and 3 experimental runs for monkeys T, B and R, i.e., the same runs that were used in the motion analysis in Fig. 4D.

Fig. 5C shows the time-course of z-score normalized BOLD signals in one representative voxel within a cluster at the V1/V2 border which was activated by vertical wedges (blue arrow in Fig. 5B, left). The result showed that the signal strength of this voxel increased, with some hemodynamic delay, after every onset of a vertical wedge and decreased after every change to a horizontal wedge. In contrast, in Fig. 5D, the exactly opposite pattern of BOLD signal alternations was observed for a voxel within a cluster of V2/V3 border (yellow arrow in Fig. 5B, right). Comparable results were obtained for other voxels within these clusters.

Fig. 5E–G shows retinotopic responses overlayed on the flattened occipital cortices of the three monkeys. Although there were some differences in the intensity of activity among the monkeys, the patterns of neural responses to vertical and horizontal wedges revealed the boundaries of each region of early visual cortices. These results were comparable to those in a prior study in monkeys using a standard head-post method (Lafer-Sousa and Conway, 2013; Kolster et al., 2014).

Regarding the stability of fixation behavior during the meridian mapping task, Supplementary Fig. 1B illustrates the distributions of gaze positions in a representative session, in which 7 consecutive runs of the meridian mapping task were performed (monkey T, total scan time = 32 min). Although we used a 6.1° × 6.1° fixation window in this session, we could recalculate, for each run, the percentage of time during which the gaze fell within a smaller imaginary 2.0° × 2.0° fixation window, which is typically used in vison neuroscience studies. The results showed that, in this representative session, this percentage always exceeded 96 % in all of the seven runs except for the first run (94.6 %). In this analysis, the center of the imaginary 2.0° × 2.0° window was slightly shifted rightward, (x, y) = (0.4°, 0°), relative to the screen center to match the peak of the distributions of gaze positions of this monkey. This is because this monkey has developed a habit of gazing at the right edge of the FP over the course of the experiment. Therefore, we calculated the peak of the gaze distribution during fixation across all sessions and used this value as the center of the imaginary 2.0° × 2.0° fixation window. Because the purpose of this analysis is to check for the stability of fixation, it should not be a problem to slightly shift the position of the imaginary fixation window according to the monkey's habit.

Similar trends were observed across all sessions in the three monkeys that were used to generate brain activity maps in Fig. 5E–G (19, 7 and 3 runs were conducted in monkeys T, B and R, respectively). The percentage of time during which the gaze position fell within the imaginary 2.0° × 2.0° window was 95.4 ± 1.2%, 93.7 ± 2.4% and 84.5 ± 2.3% in monkeys T, B and R, respectively (mean ± SD). In monkeys B and R, relative to the FP, the center of the imaginary 2.0° × 2.0° fixation window was slightly shifted: (x, y) = (0.6°, 0°), and (x, y) = (0.4°, −0.8°), respectively. These results indicate that, in the present method, problems of instability in eye measurement (e.g., drift or sudden jump of gaze position beyond several degrees caused by a loose head restraint) did not occur.

4.5. Upper limit of scan duration using masks

In the present report, the average scan duration across all sessions in the three monkeys (148 sessions) was 19.6 ± 7.4 min. (mean ± SD). The reason why we did not usually scan our monkeys longer than 30 min was not because the plastic mask cannot provide strong head-restraint for more than 30 min. Rather, this was because we wanted to terminate the scan before even a slight trend in the increase of body and head movement became evident. As is widely known, repeatedly terminating the experiment after the monkeys had begun to move would have reinforced the association that movement would allow them to return to the cage, which in turn would reinforce their body movements in the scanner. We hoped to avoid this from happening in our experiments. In addition, we usually scanned several monkeys in one session. Despite the relatively short scan duration for each monkey, we performed many sessions to obtain a total measurement time.

However, to further support the usefulness of the present method for scans of at least an hour, we selected three sessions, from the longest to the third longest, and assessed if the plastic mask could withstand being worn for 30–60 min without showing even a slight trend in the increase of head movements. These three sessions were a session comprised of 7 consecutive runs of the meridian mapping task (272 s/run, total scan duration = 32 min) (termed "Session 1″, Supplementary Figs. 1A and 2A), a session comprised of 9 consecutive runs in the free-viewing task with natural movie clips (360 s/run, total scan duration = 54 min) (termed "Session 2″, Supplementary Fig. 2B), and a session comprised of 6 runs of the free-viewing task (360 s/run) and 4 runs of a continuous fixation task (272 s/run) with various visual stimuli presented in the periphery (total scan duration = 54 min) (termed "Session 3″, Supplementary Fig. 2C). Session 1 is the same session in which the eye movement data shown in Supplementary Fig. 1B were obtained.

As shown in Supplementary Fig. 1A, in Session 1, throughout the seven runs of the meridian mapping task, the monkey's head was kept highly stable, with cumulative translational movements well below 0.50 mm in all of the seven runs. Notably, the quality of the head restraint was not deteriorated at all in the seventh run, indicating that there was no increasing trend in the frequency of head movements after 30 min of continuous fixation performance. If we consider the head-restraint situation on the final, 7th run, it is likely that scanning could have continued for a few more runs. Summary data for these 7 runs are shown in Supplementary Fig. 2A as a relative frequency histogram of relative head movements (the same format as in Fig. 4C–E). This

histogram had a mode value of 0.029 mm and a positively-skewed tail showing an almost complete absence of relative head movements greater than 0.20 mm throughout the session, which indicates that the plastic mask can tightly restrain a monkeys' head for scans longer than 30 min.

The results in Sessions 2 and 3 further supported this view. Supplementary Fig. 2B,C shows, from left to right, relative frequency histograms of head movements for the first, second and final 3 or 4 runs (18 min each) in Sessions 2 and 3 (Supplementary Fig. 2B, and **C**, respectively). In both sessions, the three histograms corresponding to the first, second and final 3 or 4 runs are almost identical in shape, with mode values of 0.026 mm, 0.027 mm and 0.026 mm for Session 2 and 0.027 mm, 0.035 mm and 0.030 mm for Session 3. Again, head movements greater than 0.20 mm were almost completely absent in both sessions, which confirmed that there were no signs of deterioration in head stability throughout these 54-min scans. Together, these results suggest that the present method is suitable for functional scans of up to at least an hour.

5. Discussion

Use of a commercially available, standard thermoplastic splint material enabled us to easily make form-fitted masks for effective head restraint of monkeys during a fMRI scan. Compared to existing standard invasive methods using a head-post and dental cement, the present method has several advantages: (1) the plastic mask is easy to make (no surgery required) and the shape of the mask can be somewhat changed afterward to improve fit and effectiveness; (2) there is no risk of infection after installation; (3) the monkey's skull and scalp are kept in a completely intact state, allowing measurements to be made without interference from implants to the signal; (4) minimal chair modifications are required to install the mask; in the present report, we only needed to add four screw holes; (5) the cost and time required to implement this method are both low.

Two to three ready-to-use plastic masks can be made within a single anesthesia session (about 30–40 min), without any invasive procedures (Fig. 1A–G). Because no post-operative recovery period is required, researchers can proceed to the next step (fitting of the mask and chair training under head restraint) within a few days after the mask is made. Through trial-and-error, we identified two critical locations on the skull for optimal head restraint during a fMRI scan: the zygomatic bones and the occipital ridge (Fig. 1H, arrows). If the mask does not fit well in these areas after it has been made, it is still possible to improve the fit of the existing mask by heating the area with a soldering iron to melt only that part of the mask and then reshaping it or attaching a new piece of softened material. In standard fMRI experiments in awake monkeys, researchers use a non-magnetic head-post to restrain head movements. This invasive technique has the risk of infection at the area of contact between skin and dental cement, as well as around anchor bolts implanted on the skull. The present technique requires no invasive procedures and no chronically implanted materials, resulting in no risk of infection. The present approach improves 'refinement' of the 3R's in animal research by minimizing the monkey's pain and distress.

In previous studies, plastic masks similar to ours have been used in monkeys in neurophysiological recording and transcranial magnetic stimulation (Drucker et al., 2015). In addition, in several previous neurophysiological studies from our group (Kadohisa et al., 2020; Watanabe et al., 2023; Stroud et al., 2023 in press), we have collected both spiking and LFP data using plastic masks that were made of the exact same material used here (i.e., the same model number from the same company). Therefore, after the fMRI measurements, one should be able to move on to neuronal recording experiments by simply cutting the area where the chamber will be implanted with scissors, taking into account the amount of dental cement around the chamber.

In one report on fMRI methodology in monkeys, a plastic helmet was combined with suction of the monkey's scalp (Srihasam et al., 2010). Suction of the scalp was applied through two holes made on both sides of the helmet to achieve further stabilization. Although this helmet showed good head-restraint performance, comparable to that in the standard head-post method, it appears to be a lot of work to create this helmet, including the preparation and maintenance of the suction mechanism. In the present study, we extended these previous results and demonstrated that, if the plastic mask is correctly shaped at a few key areas around the head (i.e., the zygomatic bones and the occipital ridge, Fig. 1H), it can by itself sufficiently suppress the monkey's head movements in awake fMRI scans. Thus, the present plastic mask has the advantages of being inexpensive, easy to make, and simple to mount on monkeys in daily sessions, requiring only about a minute at most. Another advantage is that the mask does not limit coil-shape options (Fig. 1I).

Nevertheless, the present technique has at least two limitations. First, as we noted above, although we have demonstrated that the present method is suitable for functional scans of up to at least an hour, we have not tried scans much longer than an hour. Thus, additional studies will be needed to determine whether the plastic mask can be used in fMRI experiments using a contrast agent such as monocrystalline iron-oxide nanoparticles (MION) (Vanduffel et al., 2001), which usually last several hours. Second, head movements induced by changes in body posture or those that the monkey intentionally makes of its own volition are difficult to suppress using this mask. According to our observation, such head movements are sometimes greater than 1 mm. However, if the monkey used in an experiment does not often show these behaviors, this should not be a critical issue. In fact, in the present study, our monkeys rarely showed such large, abrupt head movements even without any special, additional training to reduce body movements during a scan. In the present study, head movements greater than 1 mm were limited to less than 1.1 % of the number of volumes recorded in the latest 30 runs for the three monkeys (Fig. 4F–H). Certainly, the present method is ineffective for monkeys who have a habit of moving their bodies frequently in the scanner, and for monkeys that do not like head restraint and do not stop resisting, but this issue also applies to a standard head-post. To conclude, the present, easy-to-make plastic mask has a strong potential to simplify fMRI experiments in awake monkeys, while the obtained data are as good as or even better quality than those with the conventional head-post method.

Funding

This project was supported by Research Fellowship for Young Scientists from the Japan Society for the Promotion of Science (JSPS) (JP22J20858 and JP22KJ2205) to R.T., Grants-in-Aid for Scientific Research from the JSPS to K.W. (21K03141) and H.B. (21H00968), ERATO JPMJER1801 to H.B., and Grants-in-Aid for Scientific Research from the Japanese Ministry of Education, Culture, Sports, Science and Technology (MEXT) to S.K. (18H05522, 21H04896, 23K17462). The Japanese monkeys used in this experiment were obtained from the National Bioresource Project (Japanese Monkeys) supported by MEXT.

Data and code availability statement

The raw data and codes that support the findings of this study are openly available in the OSF repository at: https://osf.io/qpw8j/.

CRediT authorship contribution statement

Reiji Tanaka: Conceptualization, Investigation, Formal analysis, Writing – original draft, Writing – review & editing, Funding acquisition. **Kei Watanabe:** Conceptualization, Investigation, Formal analysis, Writing – original draft, Writing – review & editing, Funding acquisition. **Takafumi Suzuki:** Methodology. **Kae Nakamura:** Methodology. **Masaharu Yasuda:** Methodology. **Hiroshi Ban:** Methodology, Resources, Software, Writing – review & editing. **Ken-ichi Okada:** Methodology, Resources, Writing – review & editing. **Shigeru Kitazawa:**

Conceptualization, Writing – original draft, Writing – review & editing, Funding acquisition, Supervision.

Declaration of Competing Interest

The authors declare that there are no competing financial interests.

Data availability

We have shared the link to our data/code at the Attach File step.

Acknowledgments

We gratefully acknowledge the late Prof. Yasushi Kobayashi for his advice on the selection of mask materials and preparation methods.

Supplementary materials

Supplementary material associated with this article can be found, in the online version, at doi:10.1016/j.neuroimage.2023.120479.

References

Andersson, J.L., Skare, S., Ashburner, J., 2003. How to correct susceptibility distortions in spin-echo echo-planar images: application to diffusion tensor imaging. Neuroimage 20 (2), 870–888.
Ashburner, J., 2012. SPM: a history. Neuroimage 62 (2), 791–800.
Berg, D.J., Boehnke, S.E., Marino, R.A., Munoz, D.P., Itti, L., 2009. Free viewing of dynamic stimuli by humans and monkeys. J. Vis. 9 (5), 1–15.
Czisch, M., Wehrle, R., Kaufmann, C., Wetter, T.C., Holsboer, F., Pollmächer, T., Auer, D. P., 2004. Functional MRI during sleep: BOLD signal decreases and their electrophysiological correlates. Eur. J. Neurosci. 20 (2), 565–574.
Drucker, C.B., Carlson, M.L., Toda, K., DeWind, N.K., Platt, M.L., 2015. Non-invasive primate head restraint using thermoplastic masks. J. Neurosci. Methods 253, 90–100.
Friston, K.J., Williams, S., Howard, R., Frackowiak, R.S., Turner, R., 1996. Movement-related effects in fMRI time-series. Magn. Reson. Med. 35 (3), 346–355.
Goldstein, R., Bauer, L.O., Stern, J.A., 1992. Effect of task difficulty and interstimulus interval on blink parameters. Int. J. Psychophysiol. 13 (2), 111–117.
Ito, J., Maldonaldo, P., Grün, S., 2013. Cross-frequency interaction of the eye-movement related LFP signals in V1 of freely viewing monkeys. Front. Syst. Neurosci. 7, 1–11.
Kadohisa, M., Watanabe, K., Kusunoki, M., Buckley, M.J., Duncan, J., 2020. Focused representation of successive task episodes in frontal and parietal cortex. Cereb. Cortex 30 (3), 1779–1796.
Kolster, H., Janssens, T., Orban, G.A., Vanduffel, W., 2014. The retinotopic organization of macaque occipitotemporal cortex anterior to V4 and caudoventral to the middle temporal (MT) cluster. J. Neurosci. 34 (31), 10168–10191.
Ku, S.P., Tolias, A.S., Logothetis, N.K., Goense, J., 2011. fMRI of the face-processing network in the ventral temporal lobe of awake and anesthetized macaques. Neuron 70 (2), 352–362.
Kubilius, J., Wagemans, J., Op de Beeck, H., 2011. Emergence of perceptual Gestalts in the human visual cortex: the case of the configural-superiority effect. Psychol. Sci. 22 (10), 1296–1303.
Lafer-Sousa, R., Conway, B.R., 2013. Parallel, multi-stage processing of colors, faces and shapes in macaque inferior temporal cortex. Nat. Neurosci. 16 (12), 1870–1878.
Logothetis, N.K., Guggenberger, H., Peled, S., Pauls, J., 1999. Functional imaging of the monkey brain. Nat. Neurosci. 2 (6), 555–562.
Miyamoto, K., Osada, T., Setsuie, R., Takeda, M., Tamura, K., Adachi, Y., Miyashita, Y., 2017. Causal neural network of metamemory for retrospection in primates. Science 355 (6321), 188–193.
Oritz-Rios, M., Haag, M., Balezeau, F., Frey, S., Thiele, A., Murphy, K., Schmid, M.C., 2018. Improved methods for MRI-compatible implants in nonhuman primates. J. Neurosci. Methods 308, 377–389.
Rajimehr, R., Tootell, R.B., 2009. Does retinotopy influence cortical folding in primate visual cortex? J. Neurosci. 29 (36), 11149–11152.
Smith, S.M., Jenkinson, M., Woolish, M.W., Beckmann, C.F., Behrens, T.E., Johansen-Berg, H., Zhang, Y., 2004. Advances in functional and structural MR image analysis and implementation as FSL. Neuroimage 23, S208–S219.
Srihasam, K., Sullivan, K., Savage, T., Livingstone, M.S., 2010. Noninvasive functional MRI in alert monkeys. Neuroimage 51, 267–273.
Stroud, J.P., Watanabe, K., Suzuki, T., Stokes, M.G., Lengyel, M., 2023. Optimal information loading into working memory in prefrontal cortex explains dynamic coding. Proc. Nat. Acad. Sci. U. S. A. 120 (48), 1–12.
Tada, H., Omori, Y., Hirokawa, K., Ohira, H., Tomonaga, M., 2013. Eye-blink behaviors in 71 species of primates. PLoS One 8 (5), 1–9.
Van Essen, D.C., Drury, H.A., Dickson, J., Harwell, J., Hanlon, D., Anderson, C.H., 2001. An integrated software suite for surface-based analyses of cerebral cortex. J. Am. Med. Inform. Assoc. 8 (5), 443–459.
Vanduffel, W., Fize, D., Mandeville, J.B., Nelissen, K., Hecke, P.V., Rosen, B.R., Orban, G. A., 2001. Visual motion processing investigated using contrast agent-enhanced fMRI in awake behaving monkeys. Neuron 32 (4), 565–577.
Wandell, B.A., Dumoulin, S.O., Brewer, A.A., 2007. Visual field maps in human cortex. Neuron 56 (2), 366–383.
Watanabe, K., Kadohisa, M., Kusunoki, M., Buckley, M.J., Duncan, J., 2023. Cycles of goal silencing and reactivation underlie complex problem-solving in primate frontal and parietal cortex. Nat. Commun. 14, 5054.
Zou, Q.H., Zhu, C.Z., Yang, Y., Zou, X.N., Long, X.Y., Cao, Q.J., Zang, Y.F., 2008. An improved approach to detection of amplitude of low-frequency fluctuation (ALFF) for resting-state fMRI: fractional ALFF. J. Neurosci. Methods 172 (1), 137–141.